



FRACTURE TOUGHNESS OF INJECTION MOULDED ORGANOCLAY REINFORCED POLYPROPYLENE COMPOSITES

V. Pettarin¹, F. Brun¹, A. Pontes², J. Viana², A. Pouzada², P. Frontini^{1*}

¹ INTEMA Institute of Materials Science and Technology, University of Mar del Plata, A. Juan B. Justo 4302, B7608FDQ Mar del Plata, Argentina

² IPC/Institute for Polymers and Composites, University of Minho, Guimaraes Codex, PT4800-058, Portugal

* pmfronti@fi.mdp.edu.ar

Abstract

The fracture behavior of polypropylene reinforced with different amounts of PP/50% organoclay masterbatch was studied. Test pieces were prepared using a two-gated hot runner injection mould. Morphology of final pieces was analyzed by polarized optical microscopy, X-ray diffraction and transmission electron microscopy. Fracture toughness was evaluated under quasi-static conditions at different positions in the molded pieces. The brittle mode of failure of PP became more ductile with increasing the amount of clay. However, the mid-thickness region (core) of “ductile” samples underwent brittle fracture while the surface layers (skin) behave in a ductile way, exhibiting elongation, necking and ductile tearing, probably due to differences in thickness and crystalline structure found in skin layers of composite pieces. Different Fracture Mechanics approaches were applied to characterize the fracture behavior: fracture toughness initiation value was assessed by means of the stress intensity factor at 5% non-linearity, K_{Iq} , and fracture toughness propagation value was obtained by means of the propagation strain energy release rate, G_{cp} . It was found that fracture initiation neither depends on clay content nor on test piece location. On the other hand, clay reinforcement increased fracture propagation values away from weld line region. This toughening effect was found to be dependent on the clay content and reinforcement orientation induced by the processing technique.

1 Introduction

Injection molding is the most important process to manufacture plastic parts, since complex geometries become available in one automated production step. Nonetheless, the influence of processing parameters is critical in the performance of these products [1]. Moreover, if weld-lines are likely to occur in injection molded products, things became more complicated. Weld lines are an unavoidable reality in the injection molding of complex parts. Multiple gating, splitting of the melt flow due to inserts in the cavity or through holes, as well as changes of thickness give rise to points within the structure where the flowing fronts will recombine and weld. Weld lines are formed along with the mould filling process: particularly in the molding of very complex components a multiplicity of weld lines is generated. In weld lines, an area whose properties are different from the bulk is created [2].

Polypropylene (PP) belongs to the group of commodity thermoplastics produced in large quantities. Great efforts are undertaken to transform PP into a special thermoplastic suitable for engineering use. Research work has therefore been focused on upgrading the mechanical



performance of PP by toughening (in order to overcome the moderate cold and impact resistance) by filling and reinforcing (to increase stiffness, strength and temperature resistance and to decrease shrinkage) or both [3].

An important commodity polymer such as polypropylene (PP), when filled with a low incorporation level of nanoclay (typically less than 5%), could find ample applications in industries where requirements similar to engineering grades plastics are necessary with additional advantages [4-5]. However, only well-dispersed and well-exfoliated nanoparticles can lead to the expected improvement of properties [6-8]. Raw material producers, converters and end-users have therefore to tackle both compounding and processing issues. Surface modification of nanofillers with organic surfactant and adaptation of compounding conditions (high shear, high residence time, special screw profile design in case of melt compounding for example) may help to get rid of most of compounding issues. Research groups have made significant progress in that field. With the development of masterbatches (MB) the final injection – or extrusion – molded part should be easily obtained by mixing/diluting the MB with the appropriate polymer matrix. The nanoparticle dispersion and exfoliation is usually assumed to be achieved during the masterbatch compounding. Experience unfortunately often shows that the industrial reality is quite different [9].

Although claims are made that the mechanical properties of nanocomposites should be excellent, in practice the mechanical properties are often disappointing. In the case of the simpler mechanical properties such as Young's modulus or yield strength the testing techniques are simple and require little thought or interpretation. However, toughness is a more difficult property to characterize. Traditionally toughness has been characterized by the Izod or Charpy impact energy. It has long been recognized that the impact energy is a very complicated strain rate function of the plastic and fracture work with generally the plastic work dominating. The Izod and Charpy tests have lost favor in mechanical engineering because they cannot be used directly in design. In their desire to characterize toughness of ductile polymer nanocomposites more exactly, many researchers have turned to fracture mechanics.

Through this work fracture toughness of PP/nanoclay injected parts obtained by direct compounding of commercial PP and MB was studied under quasistatic conditions. Influence of singularities induced by processing such as weld lines and flux pattern, as well as MB content on fracture behavior was explored.

2 Experimental

2.1 Materials and processing

This study was conducted on propylene homopolymer, F-045,D2 (from SUNOCO Chemicals) blend with commercial MB of PP with 50% of organoclay, Nanomax®-PP P-802 (from Nanomax® Polyolefin Masterbatch products).

Nanocomposites were obtained by direct injection of mixtures of PP and MB. Different amounts of incorporation of nanoclays were used by diluting the 2, 6 and 10% of the MB in the PP matrix, denoted here as PP-2, PP-6 and PP-10. Rectangular boxes of 1.4 mm thickness (Fig.1) were injection molded in a double-gated hot runner injection mold by using a Klöckner Ferromatic FM20 injection machine having a 200 kN clamping force. Settings listed in table 1 were used for producing the moldings.



Morphology of moldings was analyzed by polarized light microscopy (POM), X-ray diffraction (XRD) and transmission electron microscopy (TEM). 15- μm thick specimens were microtomed with a Leitz 1401 microtome and observed with an Olympus BH2 polarized light microscope. XRD analysis was performed on pieces surface using a Phillips X'PERT MPD diffractometer (CuK α radiation $\lambda=1.5418 \text{ \AA}$, generator voltage=40 kV, current=40 mA). Measurements were recorded every 0.02 θ for 1 s each varying 2 θ from 2° to 40°. TEM microphotographs were obtained from a TEM Jeol 100 CX microscope using an acceleration voltage of 200 kV. Samples were ultramicrotomed at room temperature with a diamond knife to a 70nm thick section.



Figure 1. Hot runner mold, PP/nanoclay moldings and scheme of moldings with their dimensions.

Processing parameter	Value	
Temperature	Zone 1	160°C
	Zone 2	185°C
	Zone 3	215°C
	Zone 4	235°C
Melt temperature	220°C	
Injection speed	350 mm/s	
Screw rotation velocity	250 rpm	
Injection pressure	50 bar	
Injection time	1	
Packing pressure / time	30 bar, 10 s	
Cooling time	15 s	

Table 1 Processing settings

2.2 Fracture tests

Fracture characterization was carried out on mode I double edge-notched tensile specimens (DENT) cut from of boxes (nominal width W was 30 mm, nominal crack to depth ratio a/W was 0.5 and nominal length S was 70 mm), at a crosshead speed of 2 mm/min and room temperature in an Instron 4467 universal testing machine. Sharp notches were introduced by scalpel-sliding a razor blade having an on-edge tip radius of 0.13 μm with a Ceast Notchvis notching machine. In order to assess influence of moldings' singularities (as flux pattern and weld lines) in fracture behavior, DENT samples were cut from different places of moldings (Figure 2).

Different Fracture Mechanics approaches were applied in order to obtain initiation and propagation values of toughness. Initiation value of fracture toughness was evaluated by means of the stress intensity factor at 5% non-linearity [10]. The load at crack initiation F_q was determined as the intercept between load curve and the line of $C+5\%$ compliance, being



C the initial compliance of load-displacement curve. Stress intensity factor at initiation, K_{Iq} was then determined as:

$$K_{Iq} = \frac{F_q}{B\sqrt{\frac{W}{2}}} f\left(\frac{a}{W}\right) \quad (2)$$

with B the thickness of the sample, W the width of the sample and a the length of the notch, and $f(a/W)$ the function of the notch to width that for DENT samples is:

$$f\left(\frac{a}{W}\right) = \frac{\sqrt{\frac{\pi a}{2W}}}{\sqrt{1-\frac{a}{W}}} \left[1.122 - 0.561\left(\frac{a}{W}\right) - 0.205\left(\frac{a}{W}\right)^2 + 0.471\left(\frac{a}{W}\right)^3 + 0.19\left(\frac{a}{W}\right)^4 \right] \quad (3)$$

In addition to the stress intensity factor at initiation, the propagation value of the strain energy release rate G_{cp} was calculated from the total fracture energy U_{tot} as follows [11]:

$$G_{cp} = \frac{U_{tot}}{B(W-a)} \quad (4)$$

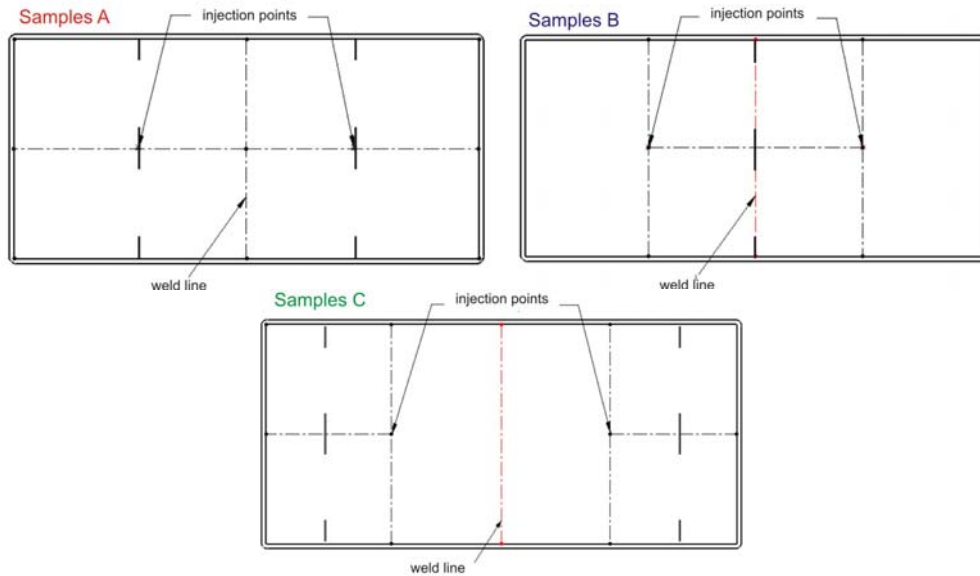


Figure 2. Location of DENT samples. Samples A: in the line of injection point. Sample B: in the weld line. Samples C: away from the injection point

3 Results and Discussion

3.1 Moldings morphology

Typical skin-core structure was found in moldings as revealed by TOM (Fig. 3a). A decrease in of the skin thickness with the increase in MB content was found (Fig 3b). Also XRD patterns indicated differences in crystalline structure of skin layer, as intensities of peaks corresponding to α -PP phase change with clay content (Fig 4.a).

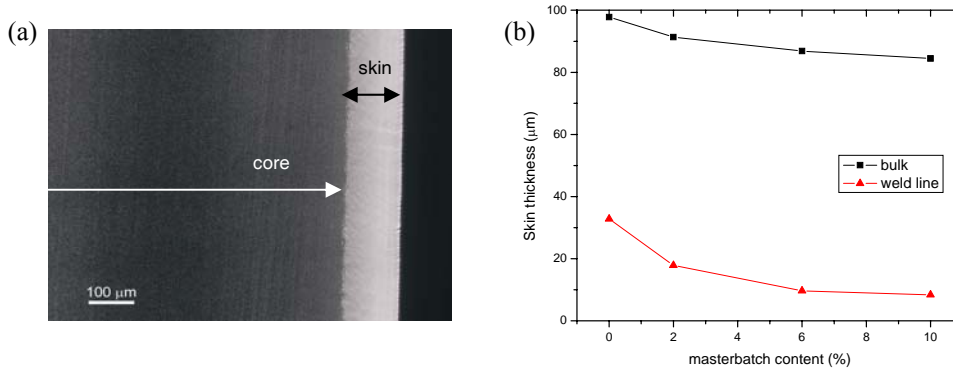


Figure 3. Optical microscopy results (a) Typical skin-core structure seen in moldings (b) Skin thickness as a function of masterbatch content

XRD patterns indicated that clay platelets are only intercalated (Fig. 4.b), while in TEM pictures clusters of stacked sheets are clearly seen (Fig. 5). This is because the degree of clay dispersion not only depends on the affinity and compatibility of the organoclay with the matrix (which is an intrinsic factor dependent on the materials), but also on the shear stress (which is an extrinsic factor dependent on processing conditions and clay loading) [12]. Hence, the fact that, in our case, organoclay exfoliation is not complete is in part because the imposed processing conditions do not generate a shear force in the mix strong enough to delaminate completely the clay agglomerates.

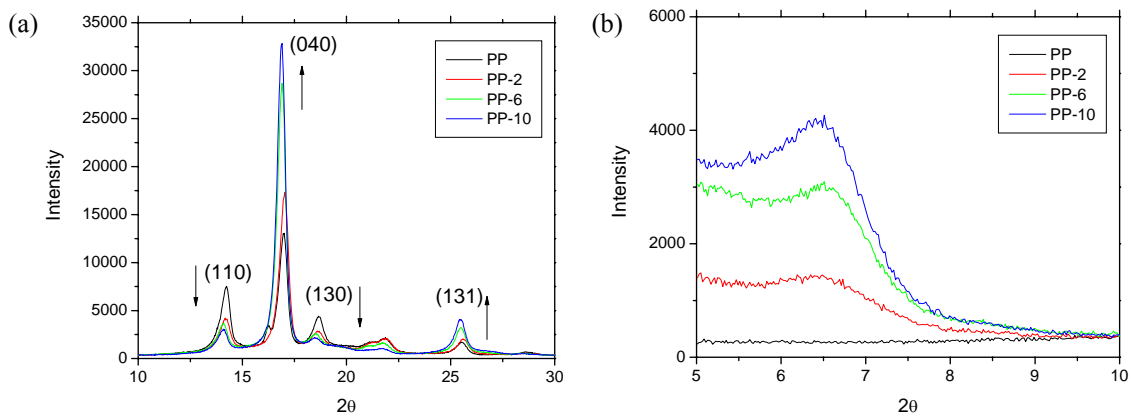


Figure 4. XRD patterns of PP/nanoclay pieces (a) high 2θ , arrows indicate changes in peak intensities of α -PP with increasing clay content (b) low 2θ

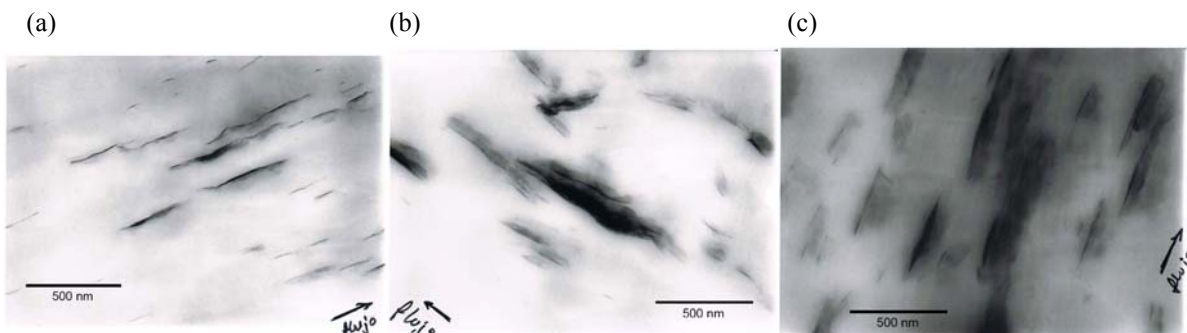


Figure 5. TEM pictures of typical PP/nanoclay pieces (a) 2% MBp (b) 6% MBp (c) 10% MBp



3.2 Fracture behavior

Typical stress-strain curves obtained for samples in different places of the moldings are shown in figure 6. PP samples underwent brittle fracture irrespective of their location in moldings (black lines in Fig. 6). The force fell almost instantaneously from the maximum force to zero, displaying very low or nil propagation energy. Further insight in the investigation of fracture performance can be acquired from the detailed inspection of the side views of the already tested DENT specimens. A typical crack propagation pattern as seen by optical microscopy is shown in Fig. 7. It is clearly observed that PP behaved in a brittle manner and crack propagated through the ligament of the specimen. However, samples did not present neat “in plane” crack propagation; the original crack was branched and deflected out of the plane that is normal to applied uniaxial tensile stress and consequently the specimen was no longer loaded in a simple mode I.

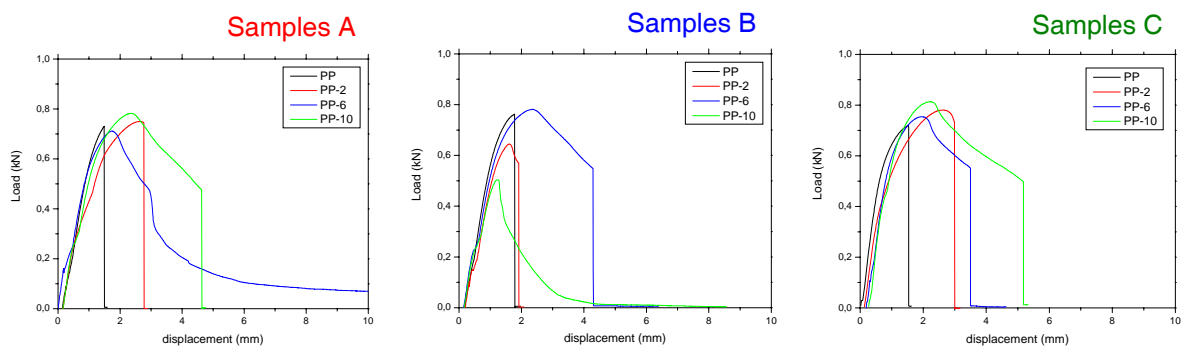


Figure 6. Typical load-displacement curves for DENT samples (a) Samples A: in the line of injection point (b) Samples B: in the weld line (c) Samples C: away from the injection point

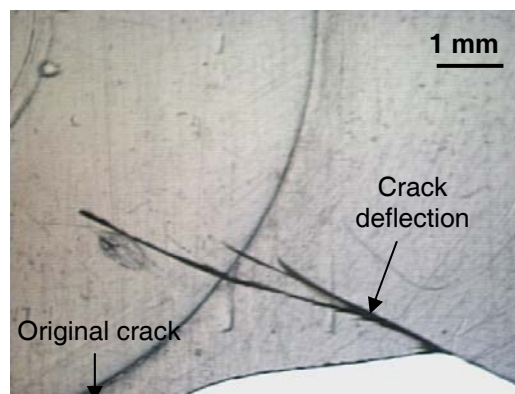


Figure 7. Side view of the fractured specimens showing crack propagation path on PP samples

PP-2, PP-6 and PP-10 present increasing ductile fracture characteristics (red, blue and green lines in Fig. 6 respectively), defined here as a fracture process that requires additional energy to propagate a crack through the specimen. A tendency toward increasing ductility and final propagation displacement were found in coincidence with the increase in MB content. Typical load displacement curves with views along the thickness in the ligament region, showing typical fracture development trough the thickness during the test are shown in figure 8.

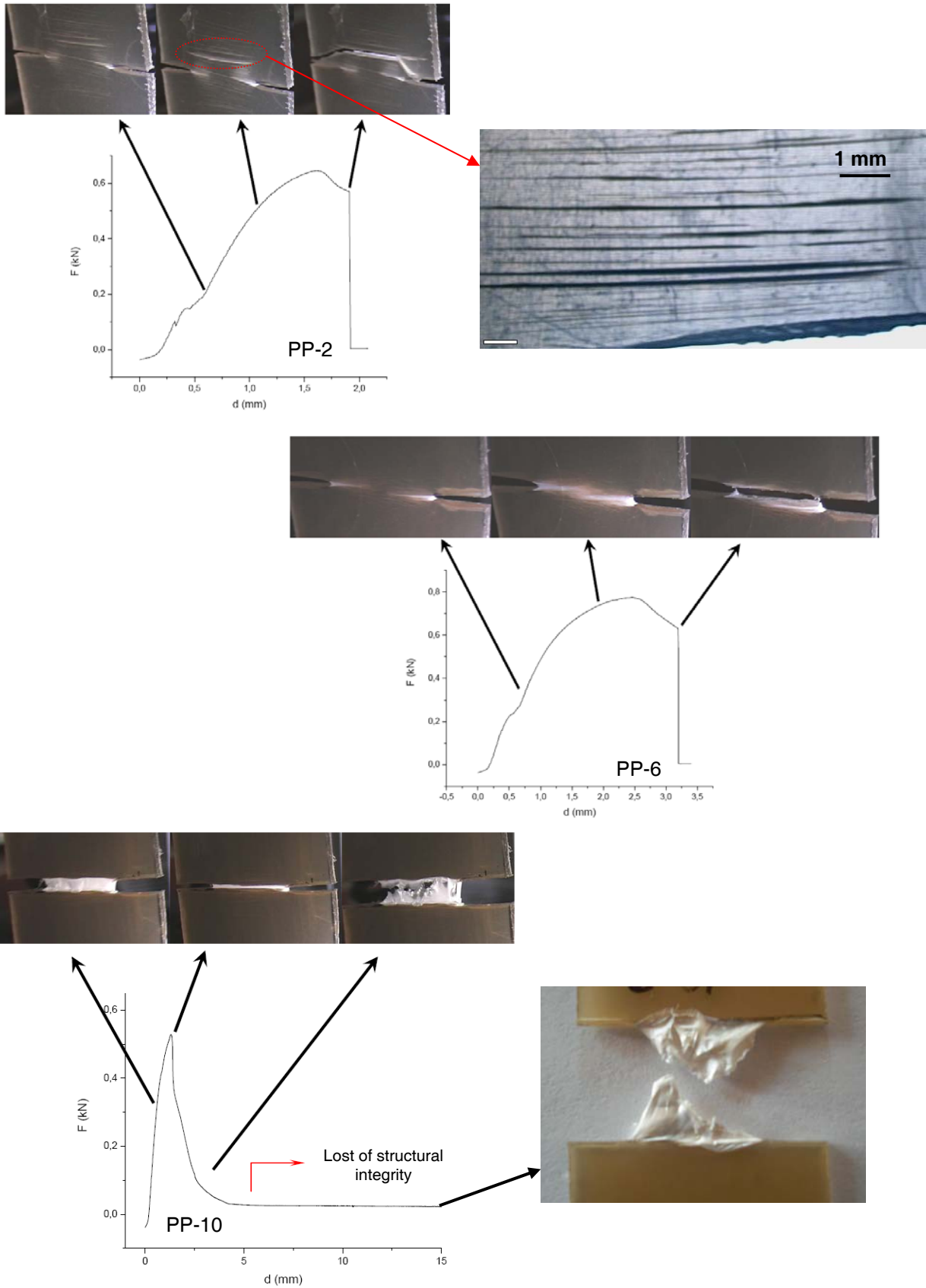


Figure 8. Typical load-displacement curves and fracture development through the thickness for nanocomposites



In nanocomposites, satellite cracks appeared and developed in planes parallel to principal crack plane. In PP-2, in which the amount of ductile deformation is small, the coalescence of these satellite cracks provoked the deflection of the original crack out of the plane that is normal to applied uniaxial tensile stress and as in PP samples the specimen was no longer loaded in a simple mode I. With increasing MB content, ductility also increases (as evidenced by whitening of ligament length). However, side views of more ductile samples show that samples had brittle fracture in the mid-thickness region, with little involvement of plastic deformation. The two halves of the specimen were still connected by the surface layers, and the further increase in displacement in load-displacement curve was caused by elongation, necking and gradual fracture of the surface layers. This effect is probably due to the differences observed in skin morphology induced by clay content.

Initiation and propagation fracture toughness values are shown in Figure 9. It is clearly seen that initiation fracture toughness value neither depend on clay content nor in location in the moldings. Also in samples containing a weld line no toughening effect was seen, indicating that weld line acted as an important defect. However, a toughening effect of clay content is seen in propagation fracture toughness of samples A and C. From a mechanical point of view there are two main potential sources of toughness in semicrystalline polymer nanocomposites: delamination or splitting of particles and matrix deformation where the major energy absorbing mechanism is the formation of multiple craze-like bands [13]. Both effects seem to be possible in our moldings: we have intercalated particles that delaminate easier than fully exfoliated platelets, and PP can undergo multiple craze. An interesting fact that should be taken into account is that the toughening effect is larger in Samples C than in samples A. This trend may result both from geometrical aspects of the part and from the filling process of the molding, as suggested by Cotterel et al [13]. It is therefore useful to recall here the uneven orientation of polymer molecules and clay platelets produced in moldings by injection molding (Fig. 10). In Samples A clay platelets are oriented parallel to the crack and they may act as defects (or voids) inducing only little craze and probably no delamination. On the other hand, in Samples C clay platelets are oriented approximated at 45° from crack line, being more effective in initiating multiple craze and particle delamination.

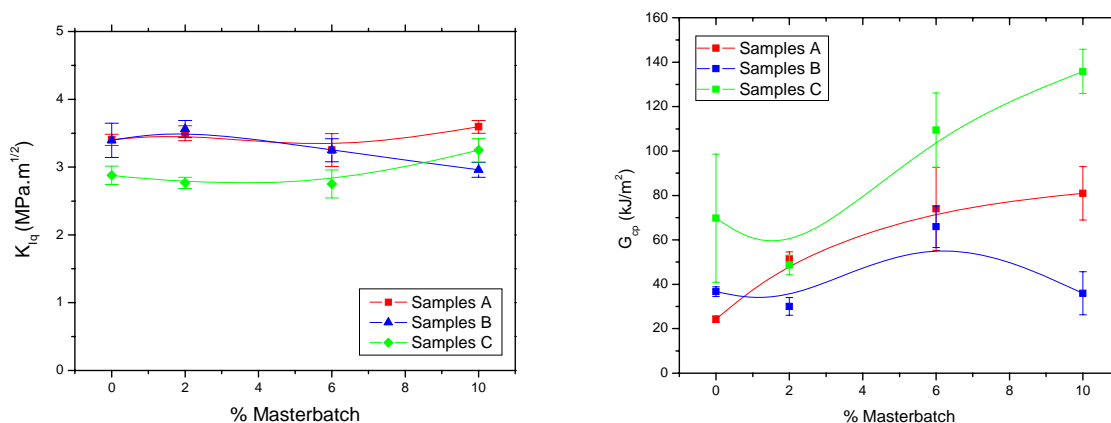


Figure 9. Stress intensity factor at initiation and energy release rate for propagation in different places of the moldings as a function of clay content

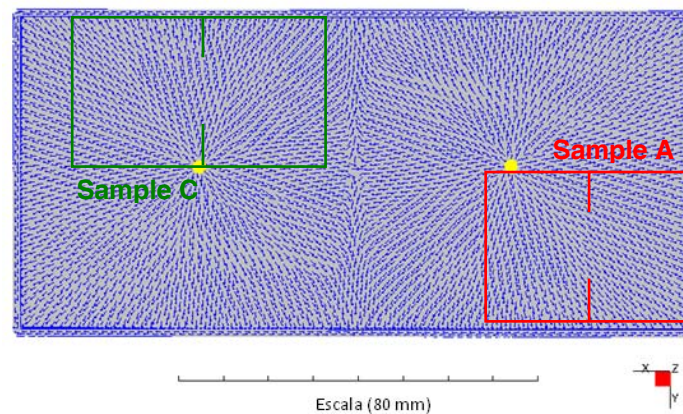


Figure 10. Orientation of polymer molecules and clay particles as assessed by Moldflow®.

This last rationalization indicates that orientation induced by processing is very important in toughness of final parts.

4 Conclusions

Through this work fracture toughness of PP/nanoclay injected parts obtained by direct compounding of commercial PP and MB was studied under quasistatic conditions. Influence of singularities induced by processing such as weld lines and flux pattern, as well as MB content on fracture behavior was explored.

PP moldings behave in the typical brittle mode of PP. Samples did not present neat “in plane” crack propagation; the original crack was branched and deflected out of the plane that is normal to applied uniaxial tensile stress and consequently the specimens were no longer loaded in a simple mode I.

A tendency toward increasing ductility and final propagation displacement were found in coincidence with the increase in MB content. Satellite cracks appeared and developed in planes parallel to principal crack plane. However, it was found that “ductile” samples underwent brittle fracture in the mid-thickness region (core) and the further increase in displacement in load-displacement curve was caused by elongation, necking and gradual fracture of the surface layers (skin). This effect was probably due to the differences observed in skin morphology induced by clay content.

Regarding fracture toughness, it was found that fracture initiation neither depends on clay content nor on test piece location. On the other hand, clay reinforcement increased fracture propagation values away from weld line region. This toughening effect was found to be dependent on the clay content and reinforcement orientation induced by the processing technique.

Acknowledgement

Authors would like to thank the National Research Council of Argentina (CONICET), the MINCyT (Argentina) and the FCT (Portugal) for financial support this research.



References

- [1] Cunha, A.M., Pouzada, A.S., Crawford, R.J., “A study of the impact behaviour of injection moulded PP using different modes of testing”, *Plast. Rubb. and Comp. Proc. Appl.*, 18, 79-90 (1992)
- [2] Ersoya OG., Nugay N., “A new approach to increase weld line strength of incompatible polymer blend composites: selective filler addition”, *Polymer* 45 (2004) 1243-1252
- [3] Karger-Kocsis J., “Instrumented impact fracture and related failure behavior in short- and long-glass-fiber-reinforced polypropylene”, *Compos. Sci. & Technol.* 48 (1993) 273
- [4] Ray and Okamoto, “Polymer/layered silicate nanocomposites: a review from preparation to processing”, *Progress in Polymer Science* 28 (2003) 1539-1641
- [5] Alexandre M., Dubois P., “Polymer-layered silicate nanocomposites: preparation, properties and uses of a new class of materials”, *Materials Science and Engineering* 28 (2000) 1-63
- [6] Zhang Y.-Q., Lee J.-H., Rhee J.M., Rhee K. Y., “Polypropylene–clay nanocomposites prepared by in situ grafting-intercalating in melt”, *Compos. Sci. & Technol.* 64 (2004) 1383
- [7] Ding C., Jia M., He H., Guo B., Hong H., “How organo-montmorillonite truly affects the structure and properties of polypropylene”, *Polymer Testing* 24 (2005) 94
- [8] Chen L., Wong S.-C., Liu T.X., Lu X.H., He C.B., “Deformation mechanisms of nanoclay-reinforced maleic anhydride-modified polypropylene” *J. of Polym. Sci. Part B: Polym. Phys.* 42 (2000) 2759-2768 Chen et al, 2000
- [9] Krawczak P., Editorial corner – a personal view, Compounding and processing of polymer nanocomposites: from scientific challenges to industrial stakes; *eXPRESS Polymer Letters* Vol.1, No.4 (2007) 188
- [10] J.G. Williams, A linear elastic fracture mechanics (LEFM) standard for determining K_{Ic} and G_{Ic} for plastics, in: C.R. Moore, A. Pavan, J.G. Williams (Eds.), *Fracture Mechanics Testing Methods for Polymers, Adhesives and Composites*,ESIS Publication 28, Elsevier, The Netherlands, 2001
- [11] MJ Adams, D Williams, JG Williams, The use of linear fracture mechanics for particulate solids, *J. of Mat. Science* 24, 1772-1776 (1989)
- [12] Dennis HR, Hunter DL, Chang D, Kim S, White JL, Cho JW, et al. Effect of melt processing conditions on the extent of exfoliation in organoclay-based nanocomposites. *Polymer* 2001; 42(23): 9513–22
- [13] B. Cotterell, J.Y.H. Chia, K. Hbaieb, Fracture mechanisms and fracture toughness in semicrystalline polymer nanocomposites, *Engineering Fracture Mechanics* 74 (2007) 1054–1078